

Simultaneous MR-PET Reconstruction using Multi Sensor Compressed Sensing and Joint Sparsity

Florian Knoll¹, Thomas Koesters¹, Ricardo Otazo¹, Tobias Block¹, Li Feng¹, Kathleen Vunckx², David Faul³, Johan Nuyts², Fernando Boada¹, and Daniel K Sodickson¹
¹Bernard & Irene Schwartz Center for Biomedical Imaging, Department of Radiology, NYU School of Medicine, New York, United States, ²Department of Nuclear Medicine, K.U. Leuven, Leuven, Belgium, ³Siemens Medical Solutions USA, New York, United States

Purpose: Current state-of-the-art MR-PET scanners enable simultaneous acquisition of PET and MR data. However, image reconstruction is usually performed separately and the results are only combined at the visualization stage. PET images are reconstructed using the Expectation Maximization (EM) [1] algorithm or one of its variants, whereas MR data are reconstructed using an inverse Fourier transform (conventional) or an iterative algorithm in cases like parallel imaging or compressed sensing. In this work we propose a new iterative joint reconstruction framework based on multi-sensor compressed sensing methods that exploits anatomical correlations between MR and PET using a joint sparsity constraint. The proposed method is tested in numerical simulations and in-vivo brain data acquired on an MR-PET scanner.

Methods: Image Reconstruction: Our approach is motivated by the idea of joint sparsity based image reconstruction of data acquired with multiple sensors [2]. While MR and PET each provide unique and independent information, they share the same underlying anatomical features. In this way information about sharp tissue edges can be transferred from the MR to the PET images. However, it is critical that features that are visible in only one of the two modalities are neither transferred to the other one nor dampened by their absence in the second modality. By treating the two imaging modalities as additional dimensions of a single dataset, the proposed method reconstructs 4D data by solution of the following optimization problem:

$$\min \|E(x_{MR}) - k\|_2^2 + EM(f, x_{PET}) + \sum_i \lambda_i \left\| \begin{array}{c} \Psi(x_{MR}^i) \\ \Psi(x_{PET}^i) \end{array} \right\|_2 + \lambda_{MR} |\Psi(x_{MR})|, \quad EM(f, x_{PET}^{n+1}) = x_{PET}^n N A^T \left(\frac{f}{A(x_{PET}^n)} \right)$$

In this equation x_{MR} and x_{PET} are the 3D image data sets, while k and f are the corresponding measured MR k-space data and PET raw data. E is the operator that maps between MR images and rawdata and also includes multiplication by coil sensitivities, i are voxel indices, Ψ is a transform to a domain where the images are sparse and λ_i and λ_{MR} are regularization parameters. EM is used to update the PET image during the iterations, A is the PET projection operator, n denotes EM iterations and N corrects for geometrical effects [1]. The forward operators also include the mapping of the two image volumes to the same resolution. In these experiments, the higher MR resolution was used. The joint sparsity term that is responsible for the exchange of anatomical information, is defined as:

$$\left\| \begin{array}{c} \Psi(x_{MR}^i) \\ \Psi(x_{PET}^i) \end{array} \right\|_2 = \sqrt{(\Psi(x_{MR}^i))^2 + (\Psi(x_{PET}^i))^2}$$

In addition to the joint sparsity term, an individual sparsity term is included for the MR dataset in order to remove undersampling artifacts. In order to avoid leakage of non-shared information from one modality to the other, we propose a spatially dependent regularization given by the difference of the signal intensities in each voxel i : $d^i = |\Psi(x_{MR}^i)| - |\Psi(x_{PET}^i)|$. The regularization parameters are then scaled down according to $\lambda_i = \lambda d^i$. This ensures that in areas where the imaged signals do not match, no joint information is shared between the two modalities. Iterative soft thresholding is used to solve the optimization problem.

Simulations: The proposed approach was first tested in simulations using the Shepp Logan phantom (128x128 image matrix). Additional structures representing lesions in the individual modalities were added to two images. For simplicity, the same resolution was used for both images. Afterwards simulated MR k-space data with a radial trajectory using 32 spokes and coil sensitivities from an 8-element head coil array were generated. Complex Gaussian noise was added to the complex k-space data. To simulate a PET acquisition, the image was forward projected to sinogram space and Poisson noise was added. The images were then reconstructed using regridding and sum of squares for MR and EM for PET, as well as with the proposed joint approach. The robustness of the joint approach against anatomical misalignment was tested by rotating the simulated PET image against the MR image by 30 degrees as well as shifting it down and to the right by 8 pixels. Wavelets were used as the sparsifying transform for the individual MR sparsity while the joint sparsity term was evaluated directly in image space (Ψ being the identity matrix in this case).

Data acquisition: MR data were acquired on a clinical 3T MR-PET System (Siemens Biograph mMR) using a conventional 12-element head coil array in CP mode. A 3D gradient echo sequence with stack-of-stars golden angle radial sampling was implemented with the following sequence parameters: TR=3.78ms, TE=1.89ms, FA=10°, 87 radial spokes per slice, each with 512 samples in the readout direction including 2-fold oversampling, matrix 256x256, FOV 220*220mm² and BW=592Hz/pixel. 58 slices were acquired in k-space with a slice thickness of 1.2mm and 6/8 partial Fourier in slice direction, which were then interpolated to 160 slices with zero filling. Images were reconstructed with regridding/EM and the joint reconstruction.

Results: Results of the simulations are shown in Figure 1. Improved image quality in terms of noise reduction, and suppression of aliasing artifacts in the case of the MR images can be observed. Neither information about misaligned edges nor information from structures that are only present in one modality, are transferred to the other image. This can also be observed in the spatially varying maps of the regularization parameter. In these plots bright values correspond to the originally defined regularization, and it can be observed that the value of the parameter is decreased whenever an image feature is only present in one of the two modalities. These findings are confirmed in the in-vivo results in Figure 2, where spatial resolution of the PET image was significantly improved without degrading the SNR.

Conclusions: Joint MR-PET reconstruction improves resolution in the PET images in regions where they are aligned with the corresponding MR image. This is in line with findings in studies using MR-based anatomical priors for PET reconstruction [3]. In regions that are highlighted in PET but without distinctive contrast in MR, e.g. next to the ventricles, the PET signal information is not improved, but also not influenced falsely by the lack of MR contrast. The proposed framework can also deal with undersampled MR data, which are improved in comparison to the gridding reconstruction mainly due to the presence of the individual sparsity term. However, it can also be observed that the MR images are not perturbed by the lower SNR and resolution of the PET data. The availability of simultaneously-acquired MR and PET data will also enable motion correction and the exploitation of dynamic correlations to be incorporated into the joint reconstruction framework, which promises to further improve image quality and enhance the information content of multimodality studies.

References: [1] Shepp and Vardi, IEEE TMI 1: 113-122 (1982) [2] Tropp et al. Proc IEEE ICASSP 2005, [3] Vunck et al., IEEE TMI 31: 599-612 (2012).

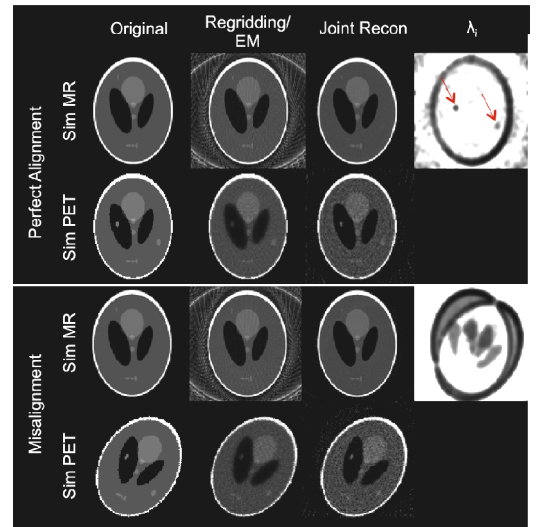


Figure 1: Simulation results for perfect alignment and misalignment between two images: Original phantoms, (first column), Regridding and EM reconstructions, the proposed joint reconstruction and the map of the spatially dependent regularization parameter λ_i . Notice the reduced values of λ_i at the positions of the additional lesions in the PET image, indicated by arrows.

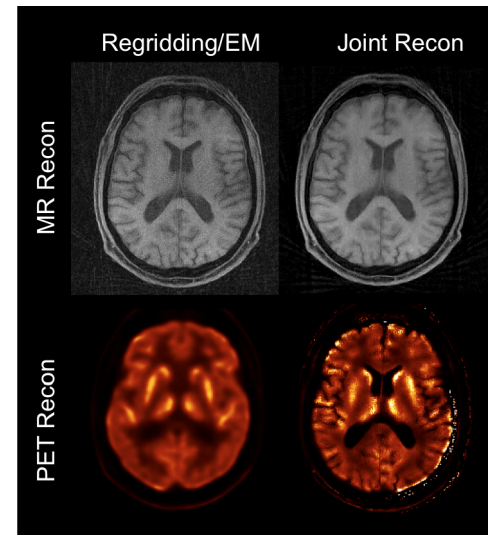


Figure 2: Regridding and EM reconstructions (left) and the proposed joint reconstruction (right) for the in-vivo brain measurements. Top: MR images. Bottom: PET images.